

Propagation of Elastic Waves in Deep Vertically Shaken Particle Beds

Alexander V. Potapov and Charles S. Campbell

Department of Mechanical Engineering, University of Southern California, Los Angeles, California 90089-1453

(Received 9 August 1996)

A wave traveling upward through a particle bed is observed to steepen and form a shock as the surface is approached. This steepening is due to the increase in the local speed of sound that is induced by the local pressure increase in the upward moving phase of the wave behind the wave front. The pressure increase leads to an increase in the local coordination number which in turn increases the local elastic modulus and the sound speed. [S0031-9007(96)01778-4]

PACS numbers: 46.10.+z, 47.50.+d, 81.05.Rm

Convection in vertically vibrated particulate systems was first observed by Faraday [1]. Since then (and especially in the last few years), vibrated particle beds and the phenomena related to these beds have been the subject of many studies, both experimental and computational [2]. However, experimental investigations are naturally limited due to the difficulties of obtaining information from deep within the bed. The computational investigations, which were most often carried out using the soft-particle discrete element method [3], have been performed mostly on shallow beds (about ten particle diameters deep), while deeper beds (of an order of several hundred particle diameters deep) have received little attention. (The only numerical investigation of a deep particle bed known to us has been carried out recently by Aoki and Akiyama [4]). There has also been many studies of the wave propagation in the granular materials (e.g., [5]); these works generally study the relatively weak sound propagation which propagates through the existing contact tree within the granular media. As the shaken bed is a dynamic situation, it opens the possibility that such contact chains may be dynamically created to suit the local conditions in the bed.

Here, we present results from a two-dimensional soft-particle [3] numerical investigation of wave propagation in a vertically shaken bed of solid particles which is approximately 1000 mean particle diameters deep. A simple linear viscoelastic response has been used in the direction normal to the contact point, and an elastic-frictional response in the tangential direction. The linear response in the normal direction is used because it generates a bulk material with an elastic modulus that have been theoretically predicted [6], and, in particular, the Young's modulus E is linearly related to the local coordination number. As a result, the elastic wave speed (proportional to $\sqrt{E/\rho_s}$, where ρ_s is the bulk density) is well defined, which, as will be seen, simplifies the interpretation of the results in that it decouples the effect of the coordination number from those of material nonlinearities. We used the same normal and tangential stiffness, K_{nt} , for all particle-to-particle and particle-to-surface contacts. The behavior of the particles subject to shaking is described by the following set of dimensionless parameters: μ , $K_{nt}/(\rho g d_0)$, e , A/d_0 and $\nu/\sqrt{g/d_0}$, where μ is the friction coefficient

between the particles, ρ is the particle density, g is the gravity acceleration, d_0 is the mean particle diameter, e is the restitution coefficient for a binary collision between particles with the diameters equal to d_0 (the parameter e characterizes the viscous dissipation), A is the amplitude of the vibration of the bottom plate, and ν is the frequency of vibration. The following values were used in these simulations: $\mu = 0.5$, $K_{nt}/\rho g d_0 = 0.142 \times 10^6$, $e = 0.8$, $A/d_0 = 0.350$, and $\nu/\sqrt{g/d_0} = 0.542$. Note that the ratio of the maximum acceleration to the acceleration of gravity is $(2\pi\nu)^2 A/g = 4.0$. For particles with a mean diameter of about 1 mm, these parameters correspond to a frequency of about 60 Hz. The choice of the contact stiffness K_{nt} was based on a desire to get a realistic bulk sound speed in the granular medium which, in loose sand, is typically about 100 m/s; the chosen properties yield that value (following the analysis in [6], based on a particle diameter of 1 mm).

In this investigation, our attention was concentrated purely on the propagation of waves caused by the interaction of a solid bottom and a bed of particles. In particular, we wished to avoid any effects of convection that might be induced by friction against the vertical walls. This is avoided by employing periodic boundary conditions on the left and right sides of the simulated region. The horizontal size of the simulation is 10 mean particle diameters, but the use of periodic boundaries approximates a system which is infinitely wide. The initial configuration of the bed is formed by placing the particles randomly in the simulated region and allowing them to settle under the influence of the gravity before shaking is started. The diameters of the particles are uniformly distributed in the range $0.8d_0 - 1.2d_0$.

Figures 1–4 show a sequence of snapshots of (a) the particle velocity, (b) wave induced normal stress (i.e., the actual stress minus the hydrostatic stress which leaves only the stresses induced by the wave passage), (c) the coordination number, and (d) the solid fraction. All are plotted as functions of position, measured in units of the mean particle diameter d_0 and referenced relative to the bottom of the bed. Time is measured in terms of the number of vibration cycles N_{cyc} , and span a complete cycle of vibration. The information here is provided for the fourth

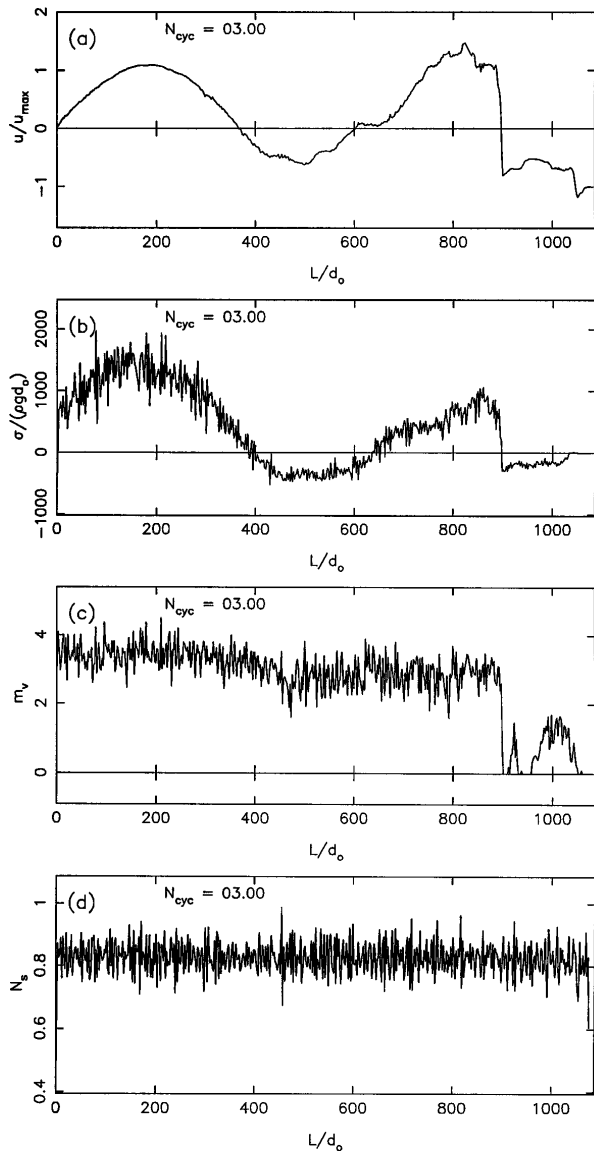


FIG. 1. The instantaneous properties in the bed as a function of the distance from the bottom of the bed L at the beginning of the third cycle of vibration ($N_{\text{cyc}} = 3.0$); (a) the particle velocity, (b) the mean normal stress caused by the propagation of the wave in the bed σ , (c) the mean coordination number for the particles in the bed m_v , and (d) the mean solid fraction of the particles N_s in the bed.

cycle of vibration only, but we have checked the repetition of the same pattern of the wave for over 20 cycles and did not see any significant differences [note the similarity of 1(a) and 4(a) in the figures which were taken one period apart]. Notice first the similarity between the shapes of the velocity and stress plots. This can be understood from the relationship between the normal stress σ and the velocity u for a flat wave in an elastic medium: $\sigma = \rho_s c_s u$, where c_s is the bulk sound speed of the material.

Also notice that the portion of the stress due to the wave propagation [plotted in Figs. 1(b)–4(b)] varies nearly sinusoidally near the base. This indicates that the material never loses contact with the bottom, but is held in place

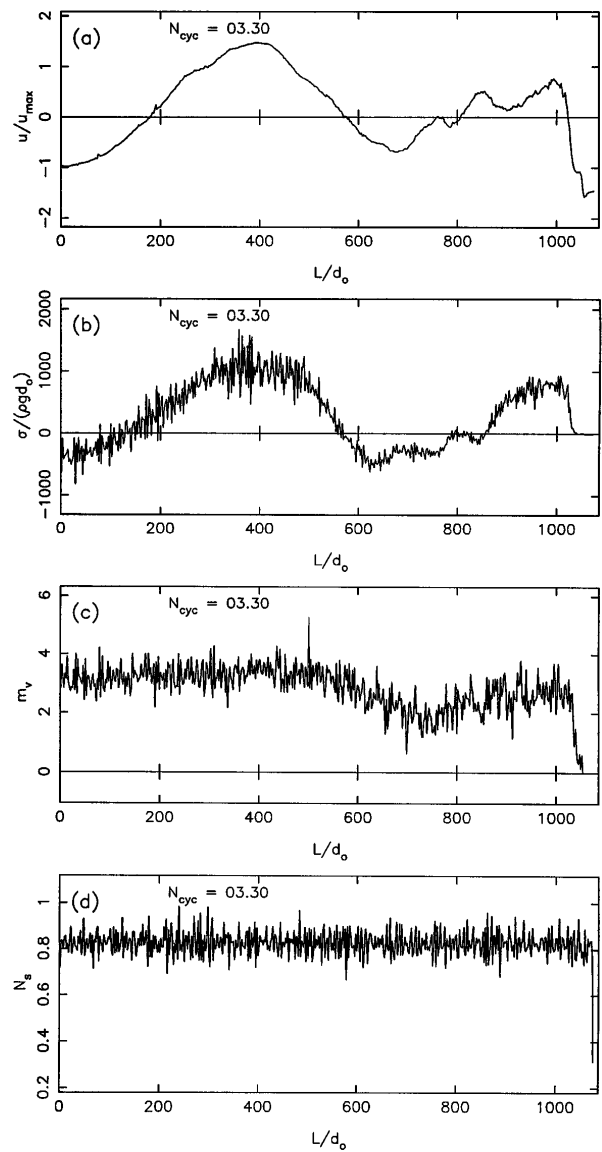


FIG. 2. The same as Fig. 1, but for $N_{\text{cyc}} = 3.3$.

by the weight of the material overburden. If the bed behaved as a rigid block, it would lose contact once the bottom acceleration exceeds the gravitational acceleration. But here, the bed must be contracting and expanding elastically so that the bed keeps contact with the plate.

Consider the velocity plots [Figs. 1(a)–4(a)]. The velocities at the beginning of the third cycle are presented in Fig. 1(a), while Fig. 4(a) corresponds to the beginning of the fourth cycle of vibration. If one follows the wave on the far left of Fig. 2(a) as it propagates upward to the right, one can see that the wave front becomes steeper as the free surface is approached. At the free surface, it becomes a shock wave with a nearly straight front. This effect is identical to the formation of the shock wave in a gas.

The similarities between these results and the formation of a shock wave in a gas go deeper than just a similarity in wave shape. Note that a shock forms in a gas because the

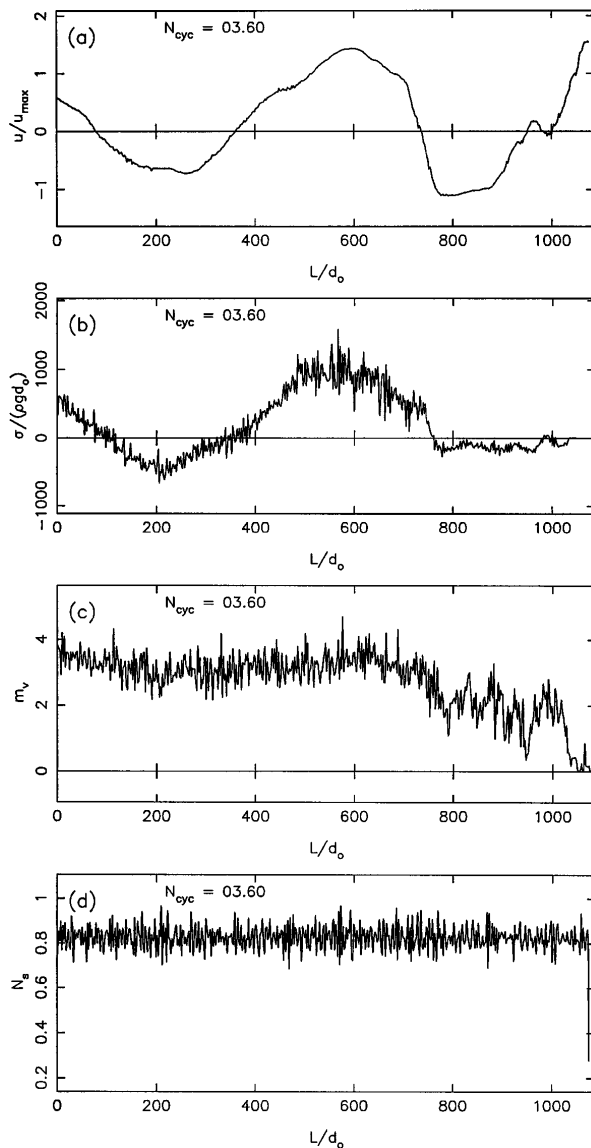


FIG. 3. The same as Fig. 1, but for $N_{cyc} = 3.6$.

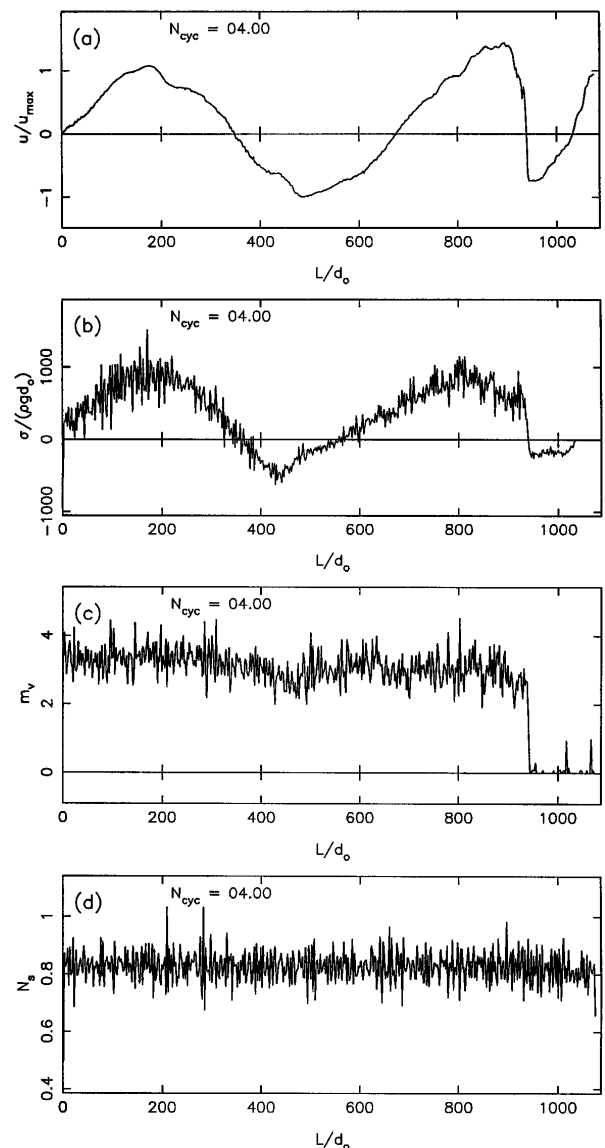


FIG. 4. The same as Fig. 1, but for $N_{cyc} = 4.0$.

temperature rises across the wave, causing the sound speed behind the wave to be larger than that in the gas before it. Here, a change in the local sound speed is also responsible for the shock formation, but, in this case, the sound speed changes due to an increase in the elastic modulus that accompanies a dynamically changing coordination number. Figures 1(c)–4(c) show the coordination number m_v . The plotted values of m_v are averaged over the same cells used to determine the velocity, each of which contains about 20 particles. The scatter in the data is due to the small number of particles in the averaging volumes. Thus the change in the coordination number is an indication that the material is dynamically changing the contact trees through which force is propagated in granular materials. (While seldom discussed in vibrating box studies, changes in the contact structure in response to applied forces has received a great deal of attention primarily in the soil mechanics community, e.g., [7].) Notice that the plots

of m_v [Figs. 1(c)–4(c)] weakly follow the trends of the normal stress [Figs. 1(b)–4(b)], in that m_v is larger in regions of large normal stress and smaller in small normal stress regions. Furthermore, the coordination number almost disappears near the free surface where the normal stresses are small. Figures 1(d)–4(d) show the mean solid fraction of the particles N_s calculated in the same manner as the mean coordination number. One can see that the solid fraction N_s changes negligibly throughout the bed and, in particular, that the changes in the normal stress induced changes in the coordination number are not reflected in the solid fraction. Thus the stress wave induces a wave in the coordination number, but with negligible change in bulk density. Furthermore, note that the solid fraction has changed little in the region near the free surface even where the coordination number has vanished.

Now, as shown in [6], the elastic modulus of a particle assembly with linear contacts is given by $E_s = m_v K_{nt} \xi / 2$

(as long as the tangential and normal stiffnesses are equal). Note that the above expression indicates that the elastic modulus is directly proportional to the average coordination number of the granular assembly. Now, the sound speed in the particle assembly varies as the square root of the elastic modulus is divided by the bulk density and multiplied by a function of the bulk Poisson's ratio. It has been shown [6] that the Poisson's ratio of an assembly of particles with linear contacts depends only on the ratio of the normal to tangential stiffness of the contacts so that, in our case, Poisson's ratio remains fixed. Also, the bulk density is directly proportional to the solid fraction N_s , which is roughly constant throughout the bed. It then follows that the local sound speed in the particle bed is directly proportional to the square root of the mean coordination number m_v . Thus, the coordination number here plays much the same role as temperature plays in the gases. As the upward moving phase of the wave passes, it increases the local value of the stresses to which the material response by setting up additional internal force chains, i.e., by increasing the coordination number. This results in a larger local elastic modulus, and, consequently, a larger local sound speed. This makes the sound speed behind the wave front larger than that before it, which results in the steepening of the wave front. The start of the steepening process may be observed deep within the bed but becomes most pronounced near the free surface where the coordination number rapidly drops to zero. Thus, very near the free surface, the elastic modulus and the sound speed likewise fall to zero. This means that the sound speed in front of the wave will go to zero as it approaches the free surface while it remains nonzero behind the front, resulting in the shock formation. Remember that the normal stresses plotted in Figs. 1(b)–4(b) show only the stresses due to the wave passage and do not reflect the hydrostatic stresses which are dominant near the bottom of the bed. Thus, near the bottom of the bed, the wave causes only a minor perturbation to the overall stress level and thus has a minor effect on the coordination number. The steepening only becomes apparent near the free surface where the wave induced stresses that are large compared to the hydrostatic forces.

Notice also that the magnitudes of the velocities increase as the wave moves up through the bed. This is because the steepening of the wave front shortens the wavelength, reducing the mass of material under each vibrational phase. Conservation of momentum dictates that the product of mass and velocity is constant so the velocity must increase as the wavelength decreases. Consequently, the particle velocities in the shock wave are large and will throw a few particles far off the bed's surface. This accounts for the low density saltated layer often observed above vibrated beds.

These results assumed a linear contact between particles (i.e., the repulsive force is linearly dependent on the particle overlap). As a result, the material possesses an elastic modulus that varies only with the coordina-

tion number. If a nonlinear stiffening contact were assumed (e.g., a Hertzian contact), the shock effect would only be intensified as the larger stresses that result in a locally larger coordination number would also induce a stiffer contact which, by itself, would increase the elastic modulus and, with it, the sound speed. We believe this effect has been seen by Aoki and Akiyama [4] who used a highly nonlinear, modified Leonard-Jones potential for their particle interaction, which gives the material complex elastic properties. (The contact model must also account for the density waves Aoki and Akiyama observed that are missing from the current results.) Although they did not specifically study the formation of the shock wave, this shock wave could be seen in their profiles on pressure and kinetic energy in the wave. Using a linear contact allows us to isolate the effects of the coordination number from any that might arise from a nonlinear contact model.

Here, we approximated an infinitely wide particle bed by employing periodic boundaries for the vertical sides of the control volume. From the above discussion, it seems clear that the same effect would be observed even if side walls were present. To check this, we ran a simulation of a wall bounded system, 30 particles wide and 300 deep, and found that the only effect on the side wall was to increase the dissipation rate of the wave's energy to sidewall friction.

This work was supported by the General Motors Corporation for which the authors are extremely grateful. Special thanks are given to Gordon Tooley

-
- [1] M. Faraday, *Philos. Trans. R. Soc. London* **52**, 299 (1831).
 - [2] J. A. C. Gallas, H. J. Herrmann, and S. Sokolowski, *Int. J. Mod. Phys. B* **7**, 1779 (1993); Y.-h. Taguchi, *Int. J. Mod. Phys. B* **7**, 1859 (1993); S. Tamura, T. Aizawa, and J. Kihara, *Int. J. Mod. Phys. B* **7**, 1829 (1993); A. Goldstein, M. Shapiro, L. Moldavsky, and M. Fichman, *J. Fluid Mech.* **287**, 349 (1995); T. Akiyama, H. Kurimoto, K. Nakasaki, and T. Matsuda, *Adv. Powder Technol.* **2**, 256 (1991); C. E. Brennen, S. Ghosh, and C. R. Wassgren, *Trans. ASME* **63**, 156 (1996); Y. D. Lan and A. D. Rosato, *Phys. Fluids* **7**, 1818 (1995).
 - [3] C. S. Campbell, *Ann. Rev. Fluid* **22**, 57 (1990).
 - [4] K. M. Aoki and T. Akiyama, *Phys. Rev. E* **52**, 3288 (1995).
 - [5] J. D. Goddard, *Proc. R. Soc. London A* **430**, 105 (1990); C. Liu and S. R. Nagel, *Phys. Rev. Lett.* **68**, 2301 (1992); C. Liu and S. R. Nagel, *Phys. Rev. B* **48**, 15 646 (1993); C. Liu, *Phys. Rev. B* **50**, 782 (1994); Y. Zhu, A. Shukla, and M. Sadd, *J. Mech. Phys. Solids* **44**, 1283 (1996).
 - [6] R. J. Bathurst and L. Rothenburg, *J. Appl. Mech.* **55**, 17 (1988).
 - [7] B. Cambou, in *Powders and Grains 93*, edited by C. Thornton (Balkema, Rotterdam, 1993), p. 73; X. Lee and W. C. Das, *ibid.*, p. 17; Y. Chen and G. Huang, *ibid.*, p. 135; L. Rothenburg and R. J. Bathurst, *ibid.*, p. 147; M. Oda, *ibid.*, p. 161.